Current-based design of metasurface antennas with tensorial surface impedance

Current-Based Design of Metasurface Antennas with Tensorial Surface Impedance

Lucia Teodorani*, Marcello Zucchi*, Giuseppe Vecchi*
*Department of Electronics and Telecommunications, Politecnico di Torino, Turin, Italy, marcello.zucchi@polito.it

***Abstract*—In this paper, a current-based algorithm for the synthesis of metasurface antennas is adapted to deal with tensorial surface impedance. The surface current is obtained through the minimization of an objective function that takes into account all constraint related to a tensorial impedance. A non-linear conjugate gradient algorithm is applied to minimize an objective function that includes both realizability and far field requirements. The proposed surface impedance distribution is then implemented through a suitable choice of anisotropic unit cells, either through local optimization or from a database of precomputed shapes. Results are shown for the case of a circular metasurface antenna radiating a linearly-polarized broadside beam.**

I. Introduction

Metasurface antennas are radiating structures based on the concept of metasurfaces, engineered two-dimensional lattices composed of a large number of subwavelength scatterers, for the control and manipulation of electromagnetic waves [1].

The design is characterized by a large number of degrees of freedom, requiring highly efficient and tailored numerical techniques. For numerical modelling purposes, the metasurface is represented with an Impedance Boundary Condition (IBC). It is well known that the radiation efficiency is higher if the surface consists of anisotropic elements, as this allows more flexibility in the control of the surface wave propagation, resulting in lower side-lobe levels and higher gain [2], [3]. Therefore, recently proposed synthesis methods have been focusing on tensorial surface impedance [4], [5].

The current-based design method introduced in [6], generalized in [7] to include realistic feeding structures, allows to design the impedance distribution without any prior knowledge of its shape (i.e., a reduced order parameterization is not required), making it particularly suitable for cases in which the profile is not known analytically, such as for synthesizing shaped beams. In the following, we will extend the method (originally formulated for scalar impedance surfaces) to allow the synthesis of tensor surface impedance profiles.

II. Synthesis of Metasurface Antennas with Tensorial Surface Impedance

A. Tensorial Impedance Boundary Condition

A locally variable tensorial Impedance Boundary Condition (IBC) relates the tangential electric field to the equivalent electric current on the surface:

$$\boldsymbol{E}_{\mathrm{t}}(\boldsymbol{r}) = \overline{\overline{\boldsymbol{Z}}}(\boldsymbol{r}) \cdot \boldsymbol{J}(\boldsymbol{r}) \tag{1}$$

in case of lossless scatterers, the impedance is purealy reactive, i.e., $\overline{\overline{\boldsymbol{Z}}} = \mathrm{j}\overline{\overline{\boldsymbol{X}}}$. In the following, we will express the impedance tensor in the local polar coordinate basis $(\hat{\boldsymbol{\rho}}, \hat{\boldsymbol{\phi}})$,

$$\overline{\overline{\boldsymbol{Z}}} = \mathrm{j}\begin{bmatrix} X_{\rho\rho} & X_{\rho\phi} \\ X_{\phi\rho} & X_{\phi\phi} \end{bmatrix} = \mathrm{j}\begin{bmatrix} X_{\mathrm{I}} + X_{\mathrm{K}} & X_{\mathrm{L}} \\ X_{\mathrm{L}} & X_{\mathrm{I}} - X_{\mathrm{K}} \end{bmatrix} \tag{2}$$

Here, the coefficient X_{I} corresponds to the *isotropic* part of the tensor, while X_{K} and X_{L} quantify the *anisotropy* of the impedance [8]. All coefficients are functions of the position on the surface.

The electromagnetic scattering problem is formulated as an integral equation (EFIE-IBC),

$$\boldsymbol{E}_{\mathrm{inc}} + \mathcal{L}\boldsymbol{J} = \overline{\overline{\boldsymbol{Z}}} \cdot \boldsymbol{J}, \tag{3}$$

where $\boldsymbol{E}_{\mathrm{inc}}$ is the incident (source) field, while $\mathcal{L}$ is the Electric Field Integral Operator. The dependence on the position has been omitted for clarity. The current is expanded as a linear combination of RWG basis function and the discretization of the problem follows the usual Method of Moments procedure with Galerkin testing.

B. Current-based IBC synthesis

The IBC synthesis is based on the framework presented in [6]. An optimization problem is formulated where the design variable is the equivalent surface current only, and the objective function to be minimized embeds all *design requirements* (pattern masks, impedance range) and *physical constraints* (passivity, losslessness) without requiring the surface impedance explicitly. The requirements are expressed as a sum of non-negative penalty functions over all cells,

$$f(\boldsymbol{J}) = \sum_{i=1}^{N_{\mathrm{c}}} \left(\rho_i^{\mathrm{phy}}(\boldsymbol{J}) + \rho_i^{\mathrm{des}}(\boldsymbol{J})\right) \tag{4}$$

where the local penalties ρ_i^{phy} encode the physical constraints, while ρ_i^{des} the design ones. All these local penalties functions are fourth-order polynomials in the current coefficients.

The function is minimized with a *non-linear conjugate gradient algorithm*, with a custom line-search procedure that fully exploits the polynomial structure of the objective function. The algorithm is applicable to large structures by exploiting common fast numerical algorithms for the computation of the scattered fields from the currents.

C. From Currents to Tensorial Impedance

To complete the design process, we need a procedure to obtain the tensor impedance from the knowledge of the optimal current $\tilde{\boldsymbol{J}} = \sum_n \tilde{I}_n \boldsymbol{f}_n$ (and of the electric field, obtained as $\tilde{\boldsymbol{E}} = \boldsymbol{E}_{\text{inc}} + \mathcal{L}\tilde{\boldsymbol{J}}$).

We can observe that, starting from the tensorial IBC (1), we need to obtain the values for the three independent degrees of freedom X_{I}, X_{K} and X_{L}. To this aim, we test (1) with the following independent testing functions:

$$\boldsymbol{\tau}_{\text{N}} = \left(\hat{\boldsymbol{\phi}}\hat{\boldsymbol{\rho}} - \hat{\boldsymbol{\rho}}\hat{\boldsymbol{\phi}}\right) \cdot \tilde{\boldsymbol{J}} = \hat{\boldsymbol{n}} \times \tilde{\boldsymbol{J}} \tag{5}$$

$$\boldsymbol{\tau}_{\text{K}} = \left(\hat{\boldsymbol{\rho}}\hat{\boldsymbol{\rho}} - \hat{\boldsymbol{\phi}}\hat{\boldsymbol{\phi}}\right) \cdot \tilde{\boldsymbol{J}} \tag{6}$$

$$\boldsymbol{\tau}_{\text{L}} = \left(\hat{\boldsymbol{\phi}}\hat{\boldsymbol{\rho}} + \hat{\boldsymbol{\rho}}\hat{\boldsymbol{\phi}}\right) \cdot \tilde{\boldsymbol{J}} \tag{7}$$

obtaining a diagonal linear system,

$$\begin{bmatrix} -\mu_{\text{N}} & 0 & 0 \\ 0 & -\mu_{\text{N}} & 0 \\ 0 & 0 & \mu_{\text{N}} \end{bmatrix} \begin{bmatrix} X_{\text{I}} \\ X_{\text{K}} \\ X_{\text{L}} \end{bmatrix} = \begin{bmatrix} p_{\text{N}} \\ p_{\text{L}} \\ p_{\text{K}} \end{bmatrix}. \tag{8}$$

The element of the matrix and of the rigth hand side are defined as

$$\mu_{\text{N}} = \operatorname{Im}\left(\tilde{\boldsymbol{J}} \cdot \boldsymbol{\tau}_{\text{N}}^{*}\right), \qquad p_{\text{N}} = \operatorname{Re}\left(\tilde{\boldsymbol{E}} \cdot \boldsymbol{\tau}_{\text{N}}^{*}\right)$$
$$p_{\text{L}} = \operatorname{Re}\left(\tilde{\boldsymbol{E}} \cdot \boldsymbol{\tau}_{\text{L}}^{*}\right), \qquad p_{\text{K}} = \operatorname{Re}\left(\tilde{\boldsymbol{E}} \cdot \boldsymbol{\tau}_{\text{K}}^{*}\right)$$

The solution of (8) is given trivially by

$$X_{\text{I}} = -p_{\text{N}}/\mu_{\text{N}} \tag{9}$$

$$X_{\text{K}} = -p_{\text{L}}/\mu_{\text{N}} \tag{10}$$

$$X_{\text{L}} = p_{\text{K}}/\mu_{\text{N}} \tag{11}$$

and the original tensor (2) can be reconstructed on each point on the surface. In the design of practically relevant metasurface antennas, we are usually interested in capacitive impedance, which is easily implementable with patterned metallic patches on the dielectric substrate. In the case of a tensorial impedance, this condition is enforced by requiring both eigenvalues of the tensor (2),

$$\xi_1 = X_{\text{I}} + \sqrt{X_{\text{K}}^2 + X_{\text{L}}^2}, \tag{12}$$

$$\xi_2 = X_{\text{I}} - \sqrt{X_{\text{K}}^2 + X_{\text{L}}^2} \tag{13}$$

to be negative. A sufficient condition is obtained by imposing

$$X_{\text{I}} < 0 \tag{14}$$

$$\left(X_{\text{K}}^2 + X_{\text{L}}^2\right) < X_{\text{I}}^2 \tag{15}$$

by substituting (9)–(11) in (14)–(15), we arrive at the final constraint formulation,

$$p_{\text{N}} > 0 \tag{16}$$

$$p_{\text{N}}^2 > p_{\text{K}}^2 + p_{\text{L}}^2 \tag{17}$$

in which all quantities depend on the surface current only and can therefore be seamlessly included in the current-based optimization by defining the associated cost functionals.

In the final step, from the computed tensor impedance values the appropriate shape of the metallic patterning for each cell in the lattice has to be defined. This can be done in multiple ways: by picking a suitable candidate from a database of pre-computed shapes (where each shape is simulated within a periodic approximation, and the corresponding impedance is extracted as in [9]), or through a cell-by-cell optimization in an aperiodic environment [10].

III. Results

The circular metasurface has been designed at a frequency of 23 GHz and has a diameter $D = 158$ mm $\approx 12\ \lambda$. An RO3003 dielectric grounded substrate with $\varepsilon_{\text{r}} = 3$ and thickness $h = 1.27$ mm has been used. The excitation is approximated as a TM_0 cylindrical surface wave supported by the grounded substrate, which represents the main contribution of the field radiated by a realistic feed (e.g., vertical conductor pin in the centre of the antenna). The surface is discretized with 41 776 RWG basis functions.

The desired broadside beam has a 10° HPBW, linear polarization along the x-axis, with cross-polarization and sidelobes levels below -25 dB. The isotropic coefficient X_{I} of the tensor impedance is constrained to be less than -200Ω, consistent with our requirement for capacitive surfaces.

Fig. 1a–1c show the synthesized tensor coefficients X_{I}, X_{K}, X_{L}, while Fig. 1d–1f show the same profile expressed in the local polar coordinate basis. The isotropic coefficient values are below the set upper bound on the entire surface, but this alone does not guarantee that the obtained solution is capacitive. Indeed, to confirm this, we can refer to the eigenvalues distributions in Fig. 2a and 2b, where it is clear that, everywhere on the surface, both ξ_1 and ξ_2 are negative.

The resulting realized gain pattern is shown in Fig. 3, together with the surface current magnitude. Both the co- and cross-polarization components comply with the requirements, with a maximum realized gain of 24 dB and a 52% aperture efficiency.

IV. Conclusions

In this work, a current-based algorithm for the synthesis of tensorial metasurface antennas has been presented. From the optimized current, it is possible to obtain the tensor impedance distribution through an appropriate local testing procedure. A linearly-polarized, broadside beam radiating MTS antenna has been designed with the proposed algorithm. The resulting impedance fulfills all requirements for a capacitive impedance profile, as highlighted by the eigenvalues distribution.

Acknowledgement

This work was supported by the European Union - Next Generation EU under the Italian National Recovery and Resilience Plan (NRRP), Mission 4, Component 2, Investment 1.3, CUP E13C22001870001, partnership on "Telecommunications of the Future" (PE00000001 - program "RESTART").

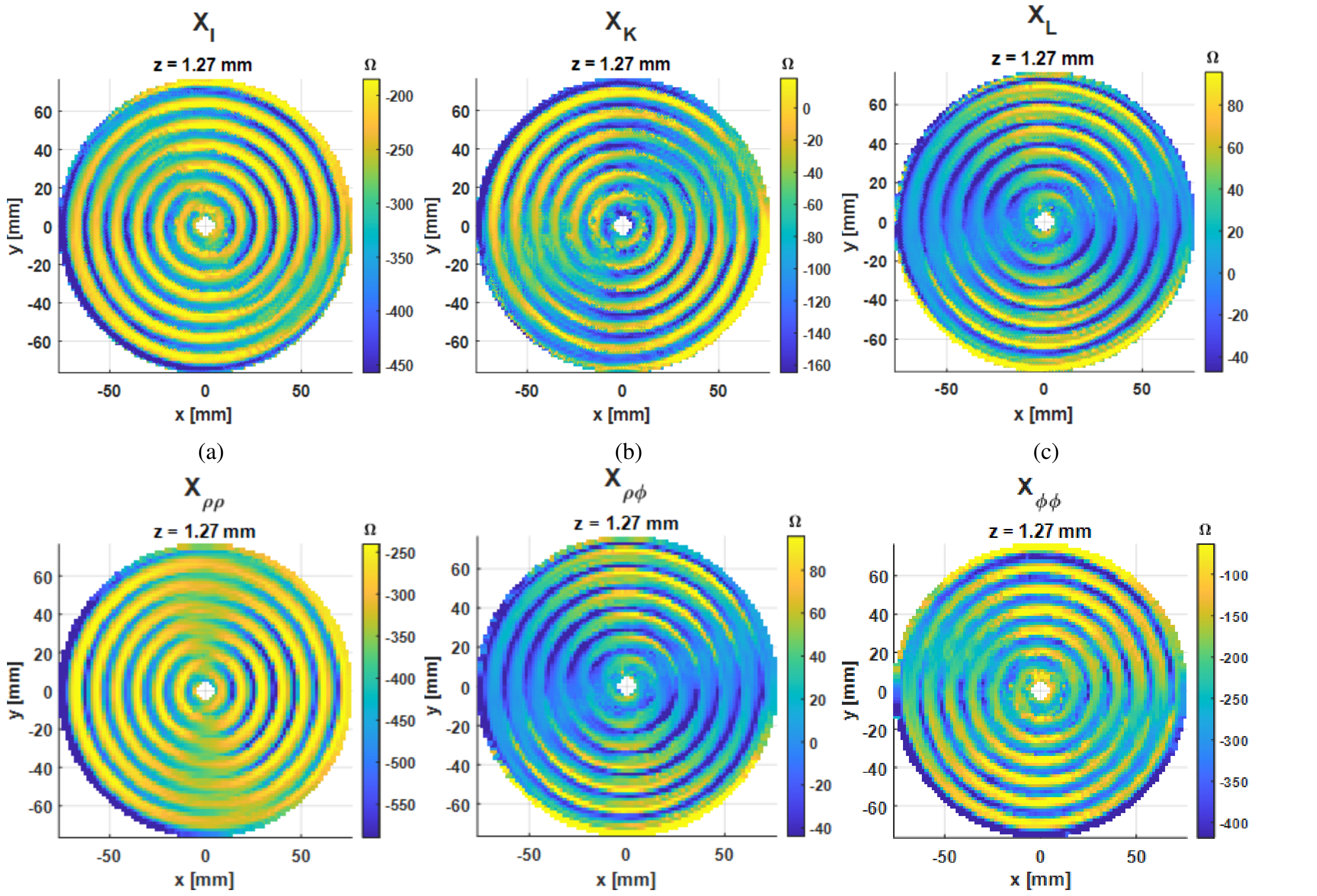

(a) (b) (c)

(d) (e) (f)

Fig. 1: Circular tensorial MTS antenna radiating a linearly-polarized broadside beam: (a), (b) and (c) synthesized surface tensor parameters, (d), (e) and (f) corresponding surface tensor components in the local polar coordinate orthogonal basis.

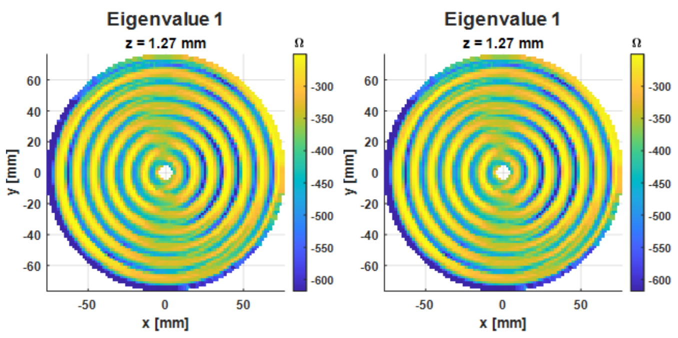

(a) (b)

Fig. 2: Eigenvalues (a) ξ_1 and (b) $\xi, 2$ of the synteshized surface tensor impedance.

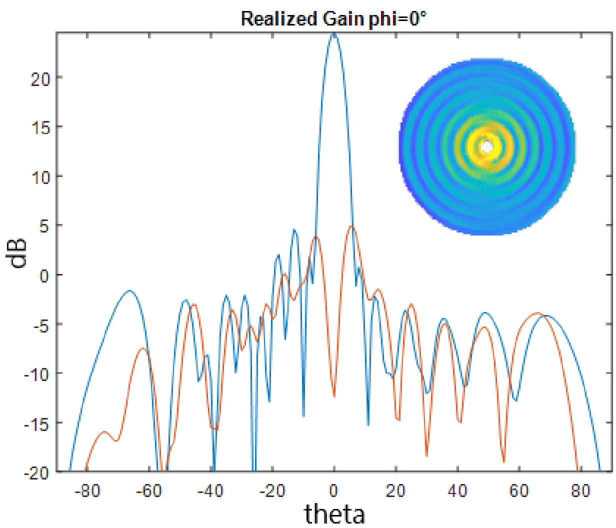

Fig. 3: Far field realized gain pattern for co-polar (*blue*) and cross-polar (*red*) in the plane $\phi = 0°$. Optimized surface current (*inset*).

REFERENCES

[1] M. Faenzi, G. Minatti, D. González-Ovejero, F. Caminita, E. Martini, C. D. Giovampaola, and S. Maci, “Metasurface Antennas: New Models, Applications and Realizations,” *Sci Rep*, vol. 9, no. 1, pp. 1–14, Jul. 2019.

[2] G. Minatti, M. Faenzi, E. Martini, F. Caminita, P. De Vita, D. González-Ovejero, M. Sabbadini, and S. Maci, “Modulated Metasurface Antennas

for Space: Synthesis, Analysis and Realizations," *IEEE Trans. Antennas Propag.*, vol. 63, no. 4, pp. 1288–1300, Apr. 2015.

[3] G. Minatti, F. Caminita, E. Martini, M. Sabbadini, and S. Maci, "Synthesis of Modulated-Metasurface Antennas With Amplitude, Phase, and Polarization Control," *IEEE Trans. Antennas Propag.*, vol. 64, no. 9, pp. 3907–3919, Sep. 2016.

[4] M. Bodehou, C. Craeye, E. Martini, and I. Huynen, "A Quasi-Direct Method for the Surface Impedance Design of Modulated Metasurface Antennas," *IEEE Trans. Antennas Propag.*, vol. 67, no. 1, pp. 24–36, Jan. 2019.

[5] S. Pearson and S. V. Hum, "Optimization of Electromagnetic Metasurface Parameters Satisfying Far-Field Criteria," *IEEE Trans. Antennas Propag.*, pp. 1–1, 2021.

[6] M. Zucchi, F. Vernì, M. Righero, and G. Vecchi, "Current Based Automated Design of Realizable Metasurface Antennas With Arbitrary Pattern Constraints," *IEEE Trans. Antennas Propag.*, vol. 71, no. 6, pp. 4888–4902, Jun. 2023.

[7] L. Teodorani, M. Zucchi, and G. Vecchi, "Generalized Deterministic Automated Design of Metasurface Antennas with 3D Feeding Structures," *IEEE Trans. Antennas Propag.*, pp. 1–1, 2024.

[8] I. Lindell, A. Sihvola, and I. Hanninen, "Perfectly anisotropic impedance boundary," *Antennas Propag. IET Microw.*, vol. 1, no. 3, pp. 561–566, Jun. 2007.

[9] A. M. Patel and A. Grbic, "Effective Surface Impedance of a Printed-Circuit Tensor Impedance Surface (PCTIS)," *IEEE Trans. Microw. Theory Tech.*, vol. 61, no. 4, pp. 1403–1413, Apr. 2013.

[10] J. Budhu, N. Ventresca, and A. Grbic, "Unit Cell Design for Aperiodic Metasurfaces," *IEEE Trans. Antennas Propag.*, vol. 71, no. 9, pp. 7387–7394, Sep. 2023.